Statistical distribution of the electric field-driven switching of the Verwey state in Fe_3O_4

2012 New J. Phys. 14 013019

(http://iopscience.iop.org/1367-2630/14/1/013019)

New Journal of Physics
The open-access journal for physics

Statistical distribution of the electric field-driven switching of the Verwey state in Fe_3O_4

A A Fursina[1,6], R G S Sofin[2], I V Shvets[2] and D Natelson[3,4,5]

[1] Department of Chemistry, Rice University, 6100 Main Street, Houston, TX 77005, USA
[2] CRANN, School of Physics, Trinity College, Dublin 2, Ireland
[3] Department of Physics and Astronomy, Rice University, 6100 Main Street, Houston, TX 77005, USA
[4] Department of Electrical and Computer Engineering, Rice University, 6100 Main Street, Houston, TX 77005, USA
E-mail: natelson@rice.edu

New Journal of Physics **14** (2012) 013019 (9pp)
Received 9 September 2011
Published 13 January 2012
Online at http://www.njp.org/
doi:10.1088/1367-2630/14/1/013019

Abstract. The insulating state of magnetite (Fe_3O_4) can be disrupted by a sufficiently large dc electric field. Pulsed measurements are used to examine the kinetics of this transition. Histograms of the switching voltage show a transition width that broadens as the temperature is decreased, consistent with trends seen in other systems involving 'unpinning' in the presence of disorder. The switching distributions are also modified by an external magnetic field on a scale comparable to that required to reorient the magnetization.

Contents

[5] Author to whom any correspondence should be addressed.
[6] Present address: Department of Chemistry, University of Nebraska-Lincoln, 525 HAH, Lincoln, NE 68588-0304, USA.

1. Introduction

Magnetite is an archetypal strongly correlated transition metal oxide, with properties not well described by single-particle band structure. Below 858 K, magnetite, which may be written as $Fe^{3+}_{A}(Fe^{2+}Fe^{3+})_{B}O_4$, is ferrimagnetically ordered, with the A and B sublattices having oppositely directed magnetizations. The moments of the five unpaired 3d electrons of the tetrahedrally coordinated A-site Fe^{3+} ions are compensated for by those of the octahedrally coordinated B-site Fe^{3+} ions. The net magnetization results from the octahedrally coordinated B-site Fe^{2+} that have four unpaired 3d electrons [1]. Upon cooling, bulk magnetite undergoes a first-order phase transition from a moderately conducting high-temperature state to a more insulating low-temperature state at what is now called the Verwey [2] temperature, $T_V \approx 122$ K. The change in electronic properties coincides with a structural transition from a high-temperature cubic inverse spinel to a low-temperature monoclinic unit cell. The nature of the ordered insulating state remains an active topic of current research [3–6]. Experiments indicate the onset of multiferroicity [7] in magnetite below 40 K [8], further highlighting the rich physics in this correlated system.

In recent years, nanostructured electrodes have been used to apply strong electric fields in the plane of magnetite films [9, 10]. Below T_V, a sufficiently large applied voltage triggers the breakdown of the comparatively insulating low-temperature state and a sudden increase in conduction [9, 10]. This is an example of the electric field-driven breakdown of a gapped state in strongly correlated oxides [11–13], similar to the Landau–Zener breakdown in classic semiconductors. The electric field-driven transition in magnetite is consistent with the expectations [13] based on such a mechanism (via geometric scaling [9, 10], lack of intrinsic hysteresis [14] and changes of both contact and bulk resistance at the transition [15, 16]). These previous experiments examined films of various thicknesses, ranging from 30 to 100 nm. No strong thickness dependence was observed in the switching properties, consistent with the applied lateral electric field at the sample surface acting as the driver of the breakdown (although thinner films showed a less pronounced Verwey transition in low-bias resistance versus temperature measurements, consistent with expectations).

Here we report studies of the statistical variations of this electric field-driven transition in Fe_3O_4 as a function of the temperature and the magnetic field perpendicular to the film surface (out-of-plane). We find that there is a statistical distribution of switching voltages, V_{SW}, that becomes broader and shifts to higher voltages when T is reduced. We discuss these trends in the context of switching kinetics in other systems exhibiting similar trends. The application of a magnetic field perpendicular to the plane of the Fe_3O_4 film alters V_{SW}, shifting the mean by several mV (several per cent) and changing its shape, within a range of fields comparable to that required to reorient the magnetization out of plane.

2. Experimental techniques

The 50 nm Fe_3O_4 (100) thin films used in the present study were grown on (100) oriented MgO single-crystal substrates as described elsewhere [17, 18]. Contact electrodes (2 nm adhesion layer of Ti and 15 nm layer of Au) were patterned by e-beam lithography on the surface of the Fe_3O_4 film. As before [9, 14], V_{SW} scales linearly with the channel length, L (the electrode spacing), implying an electric field-driven transition. Long channels ($L > 100$ nm) required large switching voltages that would alter the electrode geometry over numerous switching cycles,

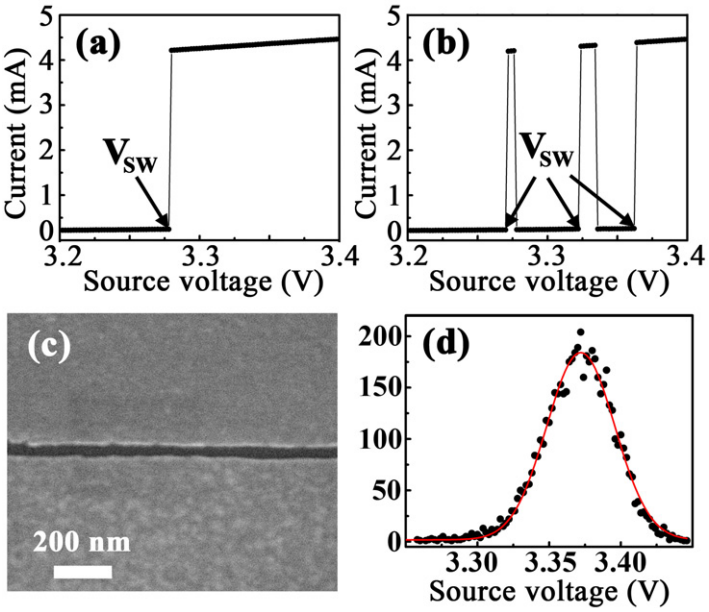

Figure 1. Details of the V_{SW} distribution experiment. (a), (b) The fragments of I–V curves in the vicinity of a transition demonstrating one (a) and three (b) switching events in a single pulsed I–V cycle. (c) Typical SEM image of Ti/Au electrodes, patterned on the magnetite film surface, separated by nanogap <100 nm. (d) An example of the V_{SW} distribution histogram at 90 K.

distorting the shape of V_{SW} histograms. To minimize V_{SW}, electrodes separated by 10–30 nm were patterned using a self-aligned technique [10]. Electrical characterization of the devices was performed using a semiconductor parameter analyzer (HP 4155A). To minimize self-heating when in the conducting state, the voltage was applied as pulses 500 μs in duration with a 5 ms period [14, 15]. The samples were cooled below T_V with no magnetic field applied, and the distribution of V_{SW} was obtained by executing several thousands of consecutive forward pulsed I–V sweeps in the vicinity of the transition point (typically the 0.2–0.3 V range) at a fixed (to within 50 mK) temperature, and recording the number of switching events at each voltage.

Each voltage value is essentially an independent test to see if switching takes place under the pulse conditions. Hence, some sweeps show one (figure 1(a)) or several (figure 1(b)) switching events. Even if the system is switched to the conducting state at $V_{SW}(1)$, it may return to the Off state between pulses and then switch to the On state at some higher voltage, $V_{SW}(2)$, and so on. The V_{SW} distribution at a particular temperature is built by recording all switching events over several thousands (3000–6000) of I–V cycles and then counting the number of switchings at a certain V_{SW}, to produce a 'number of counts' versus V_{SW} histogram. A typical V_{SW} distribution at 90 K is shown in figure 1(d). The distribution is a single peak, symmetrical around the most probable V_{SW} value.

3. Results and discussion

This procedure was repeated at each temperature below T_V ($\sim$110 K for the devices under test; see figure 2(b) inset), down to $\sim$75 K. At $T < 75$ K, the high values of V_{SW} necessarily

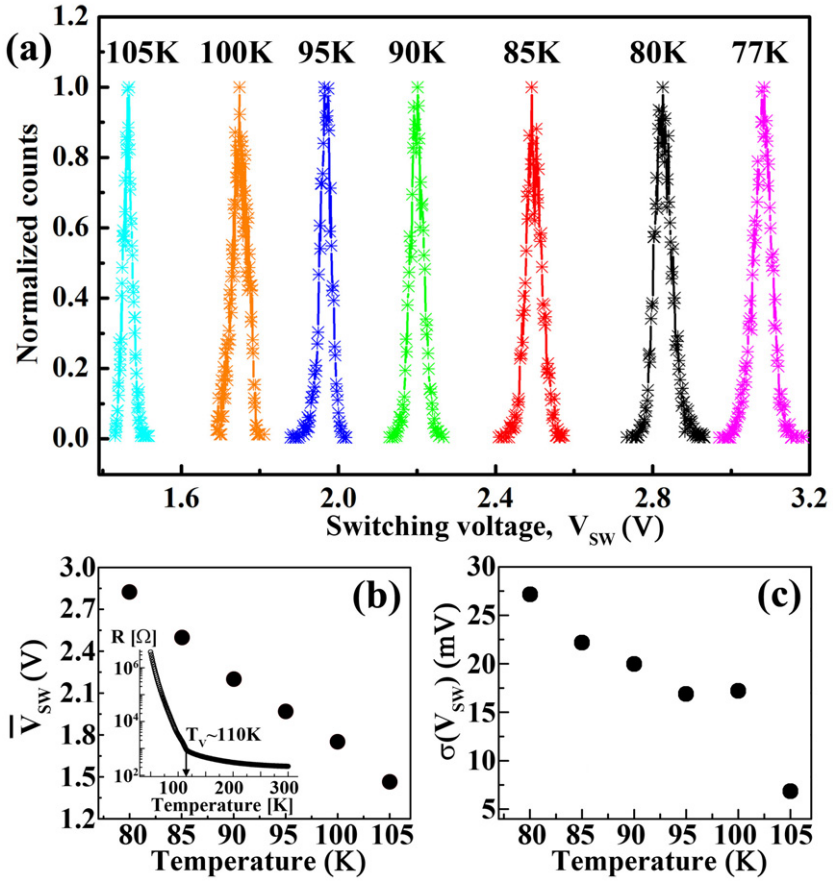

Figure 2. (a) Normalized V_{SW} distributions at different temperatures (77–105 K). (b) Temperature dependence of the mean switching voltage, $\bar{V}_{SW}$. The inset shows the zero bias R versus T plot, demonstrating $T_V \sim 110$ K. (c) Temperature dependence of the V_{SW} distribution width, $\sigma(V_{SW})$.

led to irreversible alteration of the electrode geometry, resulting in asymmetric, distorted V_{SW} histograms. As T was decreased, I–V cycles with multiple V_{SW} events (figure 1(b)) were observed more frequently. Thus, the total number of switching events observed varied with T, even with a fixed number of I–V cycles at each temperature. To compare V_{SW} distributions at different temperatures, the distributions were normalized, plotted as (the number of counts)/(max. number of counts) versus V_{SW}, where 'max. number of counts' is the number of events at the most probable V_{SW} and 'the number of counts' is the number of events at a certain V_{SW}. Figure 2(a) is an example of normalized V_{SW} distributions in the temperature range 77–105 K. The measured widths of the V_{SW} distributions are not limited by temperature stability.

As has been discussed elsewhere [14], the use of pulses is essential to minimize the role of self-heating once the system has been driven into the more conducting state. This self-heating and the short timescale [14] required to raise significantly the local temperature in the channel make it extremely challenging to determine directly whether the initial breakdown takes place through the formation of a conducting filament or through a uniform switching; once a highly conducting path is formed, the whole channel rapidly becomes conducting through self-heating. The filamentary picture is certainly likely, based on other breakdown phenomena in solids, and

the statistical variation in V_{SW} is consistent with the idea of a process involving run-to-run variability associated with *local* details rather than global material properties, but this is not definitive.

The V_{SW} distribution at each temperature is characterized by two main parameters: the mean switching value $\bar{V}_{SW} = (\sum_{i=1}^{N} V_{SW,i})/N$, where N is the total number of switching events, and the width of the distribution, calculated as a standard deviation: $\sigma(V_{SW}) = \sqrt{(\sum_{i=1}^{N}(V_{SW,i} - \bar{V}_{sw})^2)/N - 1}$. As expected, the $\bar{V}_{SW}(T)$ has the same T dependence (see figure 2(b)) as $V_{SW}(T)$ in single I–V experiments described in previous publications [9, 14]. More interesting is the $\sigma(V_{SW})$ temperature dependence, showing a broadening of the V_{SW} distribution as the temperature decreases (figure 2(c)). We note a deviation from the monotonic temperature dependence of $\sigma(V_{SW})$ at 100 K, observed in several devices tested. This is a temperature well below $T_V = 110$ K (see figure 2(b) inset), where several physical parameters (resistance, heat capacity and magnetoresistance (MR)) change abruptly.

This increase in $\sigma(V_{SW})$ as the temperature decreases is rather counter-intuitive. One might expect 'freezing' of temperature fluctuations and a decrease in thermal noise as the temperature decreases and, thus, narrowing of V_{SW} distributions. The field-driven breakdown of the insulating state is an example of the 'escape-over-barrier' problem, addressed generally by Garg [19]. Below T_V, the (temperature-dependent) effective free energy of the electronic system is at a global minimum value in the insulating state, while the external electric field modifies the free energy landscape, lowering the free energy of another local minimum corresponding to the more conducting state. As the external field is increased beyond some critical value, the minimum corresponding to the more conducting state becomes the global minimum. The nonequilibrium transition to the conducting state then corresponds to some process that crosses the free energy barrier between these minima. At a sufficiently large value of the external field, the free energy has only one minimum, corresponding to the conducting state.

As Garg showed, one may consider thermal activation over the free energy barrier as well as the possibility of quantum escape. This free energy picture predicts a broadening of the transition driving force (V_{SW} here) distribution as the absolute value of the driving force increases, consistent with our observations. This free energy picture has proven useful in studying other nonequilibrium transitions, such as magnetization reversal in nanoparticles [20] and nanowires [21, 22]. Pinning due to local disorder is one way of finding increasing distribution widths as $T \to 0$, as seen in investigations of field-driven magnetization reversal in nanowires [21, 22]. Unfortunately, quantitative modeling in this framework requires several free parameters and is difficult without a detailed understanding of the underlying mechanism.

A qualitatively similar phenomenology (a distribution of switching thresholds that broadens when T is decreased) is also observed in the current-driven superconducting–normal transition in ultrathin nanowires [24, 25]. In the latter case as in ours, self-heating in the switched state is of critical importance, as is the temperature variation of the local thermal path. Again, quantitative modeling using this self-heating approach would require the introduction of multiple parameters that are difficult to constrain experimentally, as well as detailed thermal modeling of the nanoscale local effective temperature distribution, and is beyond the scope of this paper.

We also examined the dependence of the switching distributions on the applied out-of-plane magnetic field, H. V_{SW} distributions (3000 cycles each) were collected consecutively at

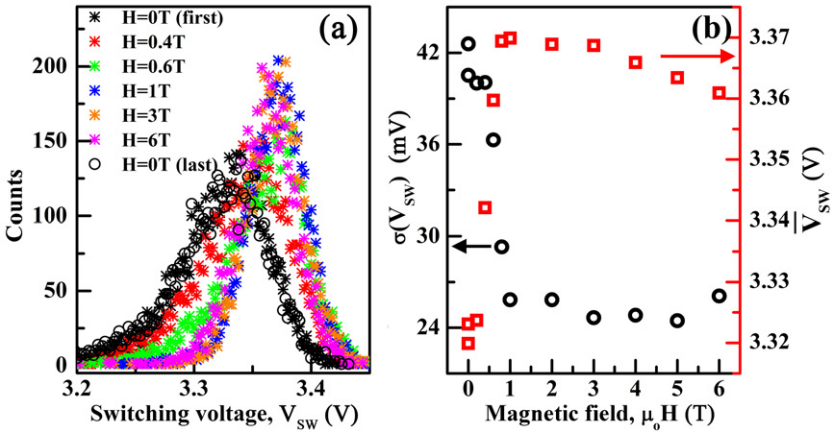

Figure 3. (a) Examples of V_{SW} distributions at selected magnetic fields ($T = 80\,K$). (b) Magnetic field dependence of the mean switching value, $\bar{V}_{SW}$ (red squares), and the width of V_{SW} distributions, $\sigma(V_{SW})$ (black circles).

12 magnetic field values: 0 T (first) → 0.2 T → 0.4 T → 0.6 T → 0.8 T → 1 T → 2 T → 3 T → 4 T → 5 T → 6 T → 0 T (last). Figure 3(a) shows the resultant V_{SW} distributions at 80 K at several selected magnetic fields. As can be seen, magnetic field shifts the V_{SW} peak to higher V values and narrows the V_{SW} distributions. To assure ourselves that the observed $\bar{V}_{SW}$ shift is not from irreversible changes in the device, a control experiment returning to $H = 0\,T$ was performed after experiments in all nonzero magnetic fields. The V_{SW} distributions at $H = 0\,T$ initially [$H = 0\,T$ (first)] and in the end [$H = 0\,T$ (last)] are identical (see figure 3(a)), meaning that the observed changes in V_{SW} distributions (shift and narrowing) are indeed caused by the applied magnetic field rather than irreversible changes to the device. Figure 3(b) quantifies the dependence of $\bar{V}_{SW}$ and $\sigma(V_{SW})$. It is clear that both parameters saturate when H is increased beyond 1 T, i.e. further increases of H up to 6 T have no significant effect. Magnetic field of the opposite polarity (not shown) has exactly the same effect on the position and width of V_{SW} distributions. Note that the shape of the distribution, in particular its asymmetry about the peak value of V_{SW}, evolves nontrivially with magnetic field, becoming more symmetric in the high field limit.

We consider whether this magnetic field dependence of the switching originates with some dependence of the bulk resistance or contact resistances, as this would alter the electric field distribution in the channel. Since V_{SW} scales with the channel length, L [9, 14], i.e. as does the resistance of the channel ($R \sim L$), one might expect that an *increase* in V_{SW} could result from an increase in the device resistance with applied magnetic field. However, Fe_3O_4 has a negative MR [23, 26, 27]. Figure 4(a) shows an example of the normalized resistance dependence, $R/R(H = 0T)$, on the out-of-plane magnetic field at 80 K. The resistance remains effectively unchanged up to ~0.4 T and then decreases as $|H|$ increases. Thus, when $\bar{V}_{SW}$ and $\sigma(V_{SW})$ experience the predominance of changes upon H application (H <1 T, see figure 3), the resistance of the device either stays constant or decreases. In the H range when R experiences significant changes (see figure 4a), $\bar{V}_{SW}$ and $\sigma(V_{SW})$ remain essentially unchanged (figure 3). Therefore, the shift of $\bar{V}_{SW}$ in the presence of H does not originate from the change in the resistance value of the device.

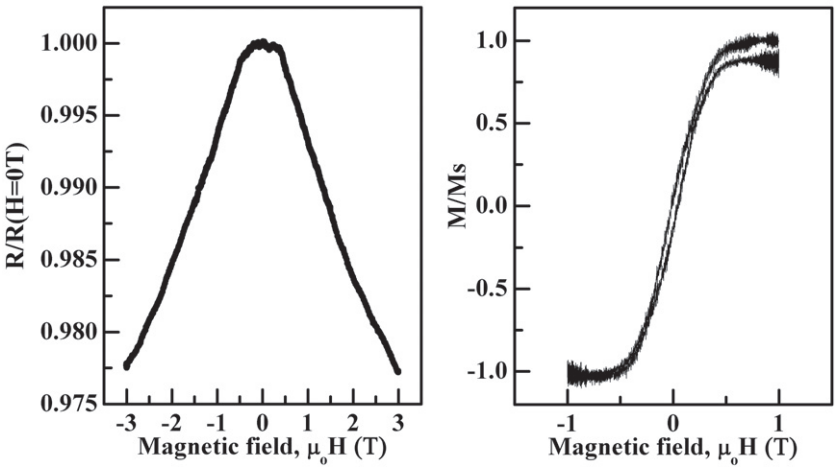

Figure 4. Dependences of the resistance ($R/R(H = 0\,T)$) (a) and magnetization (M/M_s) (b) on the out-of-plane magnetic field applied.

Another Fe_3O_4 film parameter affected by H is the magnetization of the film. Figure 4 shows the normalized out-of-plane magnetization, M/M_s, as a function of the out of plane H, where M is the magnetization of the film and M_s is the saturated magnetization. These data were consistent with previous measurements on magnetite films [28]. While we do not know the microscopic arrangement of **M** in the film in the absence of an external **H**, magnetostatic energy considerations mean that **M** under that condition lies in the plane of the film. The H range over which M is fully reoriented out of the plane (up to 1 T) matches the H range of changes in the position of $\bar{V}_{SW}$ and $\sigma(V_{SW}, T)$ (figure 3(b)). This suggests (though does not prove) that the switching kinetics parameters $\bar{V}_{SW}$ and $\sigma(V_{SW}, T)$ and therefore the stability of the gapped, low-temperature, insulating state are tied to the magnetization direction of magnetite films.

This observation is intriguing because it is not clear how the nonequilibrium breakdown of the low-temperature state would be coupled to the magnetization. Possible factors include magnetoelastic effects such as magnetostriction [29] (∼parts in 10^4 per tesla), affecting the tunneling matrix element between B-site iron atoms; and spin–orbit coupling, playing a similar role [30]. There have been reports of significant magnetoelectric and multiferroic effects in magnetite [7, 8], and a recent calculation [30] argues that these originate through the interplay of orbital ordering and on-site spin–orbit interactions of the B-site electrons. In this picture, reorientation of the spin distorts the partially filled minority-spin orbitals occupied on the B-site (formally) Fe^{2+} ions. Such a distortion would be a natural explanation for the observed correlation between **M** and the kinetics of the electric field-driven breakdown of the ordered state, which directly involves the motions of those charge carriers. It is unclear how this kind of spin–orbit physics would explain the evolution of the V_{SW} distribution, however. It would also be worth considering whether there is a correlation between the characteristics of the switching distributions reported here and the recently observed glassy relaxor ferroelectric relaxations in bulk magnetite crystals [31].

Additional, detailed experiments as a function of directionality of **H**, **M** and crystallographic orientation would be able to test these alternatives. With the existing (100) films, studies of $\bar{V}_{SW}$ and $\sigma(V_{SW}, T)$ as a function of H in the plane as well as perpendicular to the plane would be able to access the tensorial form of the H dependence. Comparison with

appropriately directed M versus H data as a function of temperature would be a clear test of whether the observed agreement between H-field scales (in V_{SW}) and reorientation of $\mathbf{M}$ is a coincidence. Further measurements on films grown with different crystallographic orientations would serve as a cross-check. It is important to note, however, that the acquisition of such data is very time-intensive due to the need to acquire many thousands of switching events. In turn, there is an accompanying requirement for extremely good device stability to avoid irreversible changes in the metal configuration over thousands of switching cycles.

4. Conclusions

We have studied the statistical distribution of the electric field needed for the breakdown of the low-temperature insulating state of Fe_3O_4. The distribution of critical switching voltages moves to higher voltages and broadens when T is reduced. This broadening is consistent with phenomenology in other nonequilibrium experimental systems incorporating disorder and thermal runaway effects. The breakdown distributions are altered by modest external magnetic fields normal to the film, suggesting the need for further experiments to understand the connection between magnetization and the breakdown of the correlated state.

Acknowledgments

The authors acknowledge valuable conversations with Paul Goldbart and David Pekker. This work was supported by the US Department of Energy grant no. DE-FG02-06ER46337. DN also acknowledges the David and Lucille Packard Foundation and the Research Corporation. RGSS and IVS acknowledge the Science Foundation of Ireland grant number 06/IN.1/I91.

References

[1] McQueeney R J, Yethiraj M, Montfrooij W, Gardner J S, Metcalf P and Honig J M 2006 Investigation of the presence of charge order in magnetite by measurement of the spin wave spectrum *Phys. Rev.* B **73** 174409

[2] Verwey E J 1939 Electronic conduction of magnetite (Fe_3O_4) and its transition point at low temperatures *Nature* **144** 327

[3] Rozenberg G K, Pasternak M P, Xu W M, Amiel Y, Hanfland M, Amboage M, Taylor R D and Jeanloz R 2006 Origin of the Verwey transition in magnetite *Phys. Rev. Lett.* **96** 045705

[4] Piekarz P, Parlinski K and Olés A M 2006 Origin of the Verwey transition in magnetite *Phys. Rev. Lett.* **97** 156402

[5] Schlappa J *et al* 2008 Direct observation of t_2g orbital ordering in magnetite *Phys. Rev. Lett.* **100** 026406

[6] Subías G, García J, Blasco J, Herrero-Martin J and Sánchez M C 2009 Resonant x-ray scattering in 3d-transition-metal oxides: anisotropy and charge orderings *J. Phys.: Conf. Ser.* **190** 012085

[7] Rado G T and Ferrari J M 1975 Electric field dependence of the magnetic anisotropy energy in magnetite (Fe_3O_4) *Phys. Rev.* B **12** 5166–74

[8] Alexe M, Ziese M, Hesse D, Esquinazi P, Yamauchi K, Fukushima T, Picozzi S and Gösele U 2009 Ferroelectric switching in multiferroic magnetite (Fe_3O_4) thin films *Adv. Mater.* **21** 4452

[9] Lee S, Fursina A A, Mayo J T, Yavuz C T, Colvin V L, Sofin R G S, Shvets I V and Natelson D 2008 Electrically driven phase transition in magnetite nanostructures *Nat. Mater.* **7** 130–3

[10] Fursina A A, Lee S, Sofin R G S, Shvets I V and Natelson D 2008 Nanogaps with very large aspect ratios for electrical measurements *Appl. Phys. Lett.* **92** 113102

[11] Asamitsu A, Tomioka Y, Kuwahara H and Tokura Y 1997 Current switching of resistive states in magnetoresistive manganites *Nature* **388** 50–52
[12] Oka T and Aoki H 2005 Ground-state decay rate for the Zener breakdown in band and Mott insulators *Phys. Rev. Lett.* **95** 137601
[13] Sugimoto N, Onoda S and Nagaosa N 2008 Field-induced metal–insulator transition and switching phenomenon in correlated insulators *Phys. Rev.* B **78** 155104
[14] Fursina A A, Sofin R G S, Shvets I V and Natelson D 2009 The origin of hysteresis in resistive switching in magnetite is Joule heating *Phys. Rev.* B **79** 245131
[15] Fursina A A, Sofin R G S, Shvets I V and Natelson D 2010 Interplay of bulk and interface effects in the electric field driven transition in magnetite *Phys. Rev.* B **81** 045123
[16] Fursina A A, Sofin R G S, Shvets I V and Natelson D 2010 Interfacial transport properties between a strongly correlated transition metal oxide and a metal: contact resistance in Fe_3O_4/M (M = Cu, Au, Pt) nanostructures *Phys. Rev.* B **82** 245112
[17] Koblischka-Veneva A, Koblischka M R, Zhou Y, Murphy S, Muücklich F, Hartmann U and Shvets I V 2007 Electron backscatter diffraction analysis applied to [0 0 1] magnetite thin films grown on MgO substrates *J. Magn. Magn. Mater.* **316** 663–5
[18] Arora S K, Sofin R G S, Shvets I V and Luysberg M 2006 Anomalous strain relaxation behavior of Fe_3O_4/MgO (100) heteroepitaxial system grown using molecular beam epitaxy *J. Appl. Phys.* **100** 073908
[19] Garg A 1995 Escape-field distribution for escape from a metastable potential well subject to a steadily increasing bias field *Phys. Rev.* B **51** 15592–5
[20] Wernsdorfer W *et al* 1997 Mesoscopic effects in magnetism: submicron to nanometer size single particle measurements *J. Appl. Phys.* **81** 5543–5
[21] Varga R, García K L, Zhukov A, Vázquez M and Vojtanik P 2003 Temperature dependence of the switching field and its distribution function in Fe-based bistable microwires *Appl. Phys. Lett.* **83** 2620–2
[22] Varga R, García K L, Vázquez M, Zhukov A and Vojtanik P 2004 Switching-field distribution in amorphous magnetic bistable microwires *Phys. Rev.* B **70** 024402
[23] Sofin R G S, Arora S and Shvets I V 2005 Study of magnetoresistance of epitaxial magnetite films grown on vicinal MgO (100) substrate *J. Appl. Phys.* **97** 10D315
[24] Sahu M, Bae M H, Rogachev A, Pekker D, Wei T C, Shah N, Goldbart P M and Bezryadin A 2009 Individual topological tunnelling events of a quantum field probed through their macroscopic consequences *Nat. Phys.* **5** 503–8
[25] Pekker D, Shah N, Sahu M, Bezryadin A and Goldbart P M 2009 Stochastic dynamics of phase-slip trains and superconductive-resistive switching in current-biased nanowires *Phys. Rev.* B **80** 214525
[26] De Teresa J M, Fernández-Pacheco A, Morellon L, Orna J, Pardo J A, Serrate D, Algarabel P A and Ibarra M R 2007 Magnetotransport properties of Fe_3O_4 thin films for applications in spin electronics *Microelec. Eng.* **84** 1660–4
[27] Eerenstein W, Palstra T T M, Saxena S S and Hibma T 2002 Origin of the increased resistivity in epitaxial Fe_3O_4 films *Phys. Rev. Lett.* **88** 247204
[28] Zhou Y, Xuesong J and Shvets I V 2004 Enhancement of the magnetization saturation in magnetite (100) epitaxial films by thermochemical treatment *J. Appl. Phys.* **95** 7357–9
[29] Tsuya N, Arai K I and Ohmori K 1977 Effect of magnetoelastic coupling on the anisotropy of magnetite below the transition temperature *Physica* B + C **86–88** 959–60
[30] Yamauchi K and Picozzi S 2010 Orbital degrees of freedom as origin of magnetoelectric coupling in magnetite arXiv:1010.1105
[31] Schrettle F, Krohns S, Lunkenheimer P, Brabers V A M and Loidl A 2011 Relaxor ferroelectricity and the freezing of short-range polar order in magnetite *Phys. Rev.* B **83** 195109